Journal of the Serbian Chemical Society
JSCS-info@shd.org.rs • www.shd.org.rs/JSCS
J. Serb. Chem. Soc. *88* (6) 627–638 (2023)
JSCS–5651
Original scientific paper
Published 17 June 2023

Physicochemical properties of the heterogeneous system Li_2CO_3–Na_2CO_3–K_2CO_3/MgO

IRINA D. ZAKIRYANOVA*, ELENA V. NIKOLAEVA and IRAIDA V. KORZUN

Institute of High-Temperature Electrochemistry, 20 Akademicheskaya Street, 620066 Yekaterinburg, Russia

(Received 1 February, revised 24 February, accepted 15 April 2023)

Abstract: The structure, conductivity, melting points and caloric melting effects of the $(Li_2CO_3–Na_2CO_3–K_2CO_3)_{eut}$ melt/MgO nanopowder heterogeneous system with MgO concentration up to 70 vol. % have been investigated. A wide variety of methods (DSC, XRD, BET, high resolution scanning electron microscope, AC impedance method, IR and Raman spectroscopy) were used to evaluate samples and research. It is revealed that at the values of effective thickness of the salt phase interlayer between MgO particles below 100 nm there is an abrupt decrease in the melting points of the salt and the normalized phase transition enthalpy of the heterogeneous system. The activation energy of the electrical conductivity rises as the values of effective thickness of the melt phase interlayer between MgO particles decreases. The study established the lack of any chemical interaction between MgO and carbonate melt at 400–600 °C. *In situ* Raman spectroscopy of the $(Li_2CO_3–Na_2CO_3–K_2CO_3)_{eut}$ melt/MgO nanopowder systems revealed the solvation of solid particles by salt-melt ions.

Keywords: molten carbonate; composite; conductivity; melting points.

INTRODUCTION

To find the optimal operating medium for the carbonate fuel cells (MCFC), the reliable physicochemical properties of heterogeneous systems based on the molten alkali metal carbonates are demanded.[1]

Molten alkali metal carbonates are chemically aggressive towards the construction materials. This fact limits their wide industrial application. Electrochemical cells with porous ceramic matrices filled with molten alkali metals carbonates are usually chosen for industrial usage.[1–4] Currently fuel cells based on binary Li/K or Li/Na molten carbonates with the γ-$LiAlO_2$ matrix are used. The operating temperature of such element is 650 °C.

* Corresponding author. E-mail: optica96@ihte.uran.ru
https://doi.org/10.2298/JSC230201023Z

The usage of the carbonate fuel cells is considered to be economically feasible in the case of at least 40000 h operation. The instability of the γ-$LiAlO_2$ phase under operation conditions is one of the major causes of the fuel cell degradation. At the temperatures above 700 °C the γ-$LiAlO_2$ modification transfers to the α-$LiAlO_2$ phase. However, with the inevitable in the MCFC operations presence of CO_2, this transfer takes place at the operation temperatures. The α-$LiAlO_2$ phase is seen to be more stable than γ-$LiAlO_2$ phase both in Li/K and Li/Na molten carbonates at 650 °C in CO_2 atmosphere.[5]

The resulting α-$LiAlO_2$ has a larger particle size than γ-$LiAlO_2$. Therefore, pore size in the matrix increase, and the mechanical strength degrade up to destruction. During the fuel cell operation the electrical conductivity decrease, and the operational performance degrade.[5]

These problems motivate the search of the materials that chemically inert to molten alkali metal carbonates and could be an alternative to γ-$LiAlO_2$.

We have previously studied the structure, conductivity and caloric melting effects of the $(Li_2CO_3–Na_2CO_3–K_2CO_3)_{eut}$ melt/α-Al_2O_3 nanopowder heterogeneous systems.[6–8] Raman spectroscopy and XRD analysis established the lack of any chemical interaction between α-Al_2O_3 and carbonate melt at 400–550 °C.

Previous articles[9–11] reported the results of the research on physicochemical properties of heterogeneous systems $(Li_2CO_3–K_2CO_3)_{eut}$ melt/CeO_2 (or α-Al_2O_3) and Li_2CO_3 melt/MgO, in which the liquid phase concentration in the studied systems is within the interval of 5 to 40 vol. %. The decrease in the relative melting enthalpy and growth of the electrical conductivity activation energy, at small liquid phase concentrations, were determined. The electrical conductivity of a Li_2CO_3 melt in a MgO matrix was compared with that in a γ-$LiAlO_2$ matrix and shown to be better.[10] Authors[10] did not prove this fact and their explanation is limited to broad terms about the influence of the solid phase on the melt conductivity.

Magnesium oxide has a stable cubic crystalline lattice (*Fm3m*) up to the melting point at 2825 °C and it is considered to be one of the most accessible and well-studied materials.

The present work is aimed at the study of the physicochemical properties of the $(Li_2CO_3–Na_2CO_3–K_2CO_3)_{eut}$ melt/MgO nanopowder heterogeneous system in order to evaluate the capability of this magnesia to be used as the filling material of the MCFC matrix**.** We focused on the study of the electrolyte conductivity, which is one of the most important characteristics of the fuel cell operation, as well as on the study of the melting point and melting enthalpy of the salt phase in heterogeneous systems. Raman spectroscopy allowed us to obtain *in situ* data on the peculiarities of the interparticle interaction and behavior of the CO_3^{2-} in the presence of the MgO nanopowder.

EXPERIMENTAL

Methods

The analysis of the phase composition of the initial salt and the frozen samples after high temperature experiments was performed using an automated X-ray diffractometer Rigaku D/MAX-2200VL/PC (Japan). The average size of the crystallites (areas of the coherent scattering) of the MgO powder was assessed using the Scherrer equation[12] and the data on the half width of diffraction peaks obtained by a diffractometer Shimadzu XRD-7000 (Japan). A certified silicon powder was used as a reference standard that denoted the instrumental input into the peak width. The samples certification on the amount of admixtures was performed using the IR absorption spectroscopy method by the IR-Fourier spectrometer Tensor 27 (Bruker, Germany). The specific surface area of the MgO powders was determined using the BET method by a SORBI (Meta, Russian Federation) device. The morphology of MgO powder was investigated by SEM (Tescan Mira 3 LMU, Czech Republic).

The melting points and the thermal effects were measured using a synchronous thermal analyzer STA 449C Jupiter (NETZSCH, Germany). The measurements were performed in pure argon atmosphere (99.998 %) at the sample heating rate of 10 K/min (Pt–Rh crucibles). The error of the phase transitions temperature measurements did not exceed 1 K. The differential scanning calorimetry (DSC) measurements of the heterogeneous system provided reproducible results, and the data on the second and the following heating of the samples were used for analysis.

Electrical resistance of heterogeneous systems, contain up to 50 vol. % of MgO, was determined *via* godograph of the impedance. AC impedance was measured under Ar atmosphere with the impedancemeter Z-1500J (Elins, Russian Federation) in a frequency range 20 Hz–1.5 MHz using platinum (Pt) electrodes. Specific electrical conductivity was calculated according to the equation: $\sigma = K/R$, where K is the cell constant (cm^{-1}), and R is the ohmic resistance of electrolyte (Ohm). The cell constant was determined using the electrical conductivity values of molten KNO_3. The cell was standardized according to the melt with the known values of electrical conductivity under the same conditions as at the experiments on the determination of the electrical resistance of the systems under study, *i.e.*, at the fixed immersion depth of the electrode into the melt, at the same interelectrode distance and in the same temperature range. At least three parallel measurements were made for each series of experiments.

Raman spectra of high temperature heterogeneous systems with MgO concentrations 23 and 70 vol. %, were recorded by a fiber optic spectrometric complex Ava-Raman (Avantes, Netherlands), which includes a source of monochromatic laser emission (50 mW, λ = 532 nm, 180° registration scheme). The spectrometer is equipped with a notch-filter, which limits intense Rayleigh scattering in the region of 150 cm^{-1}. The determination error of the wave numbers was 1 cm^{-1}. An original high temperature optic attachment was developed and successfully tested previously at the *in situ* analysis of interaction between barium oxide or lead oxide and molten alkali metal chlorides.[13,14] In this work the attachment was used to record spectra of the heterogeneous systems. A platinum crucible of the 20 mm height and 12 mm diameter was used as a container for the heterogeneous systems under study. The spectra were recorded at the temperatures above the melting point of carbonate eutectic (398 °C) in air atmosphere. The spectral characterizations are reproducible both in a series of experiments and in heating-cooling modes for the desired composition of a heterogeneous system. The presence of any interaction products of the container material (Pt) and the heterogeneous systems under study has not been detected by the XRD analysis of the frozen fusions.

Preparation and certification of the samples

Chemically pure grade Li_2CO_3, Na_2CO_3 and K_2CO_3 ("Vekton", St. Petersburg, Russian Federation) were preliminary dehydrated under vacuum at stepwise temperature growth and melted in argon atmosphere.

The carbonate eutectic mixture $(Li_2CO_3–Na_2CO_3–K_2CO_3)_{eut}$ (43.5, 31.5 and 25.0 mol %, respectively) was prepared by fusion of the weighted portions of the salts. The salts were thoroughly mixed, dried at reduced pressure at 200 °C for 1 h to remove traces of adsorbed H_2O, heated in a CO_2 atmosphere, and held for 5 h at 800 °C to obtain homogeneous molten mixture. The frozen eutectic carbonate mixture was examined by DSC analysis. The melting point (T_m = 398 °C) and the melting enthalpy (ΔH_{eut} = 277 J/g) of eutectic composition are in agreement with the published data.[15]

MgO powder (analytically pure, "Chimreaktivsnab," Ufa, Russian Federation) was confirmed to be a single phase using XRD and IR spectroscopy. The IR spectrum of MgO showed a strong broad band in the range 400–700 cm^{-1} that corresponded to Mg–O vibrations. There are no any vibration bands inherent to adsorbed water or hydroxyl groups. Magnesium oxide of different dispersity was used: average crystallites size of 95 nm and specific surface area (S) of 9.4±0.1 m^2/g; and crystallite size of 25 nm and S = 15.0±0.1 m^2/g. The morphology of MgO powder investigated by SEM is shown in Fig. 1.

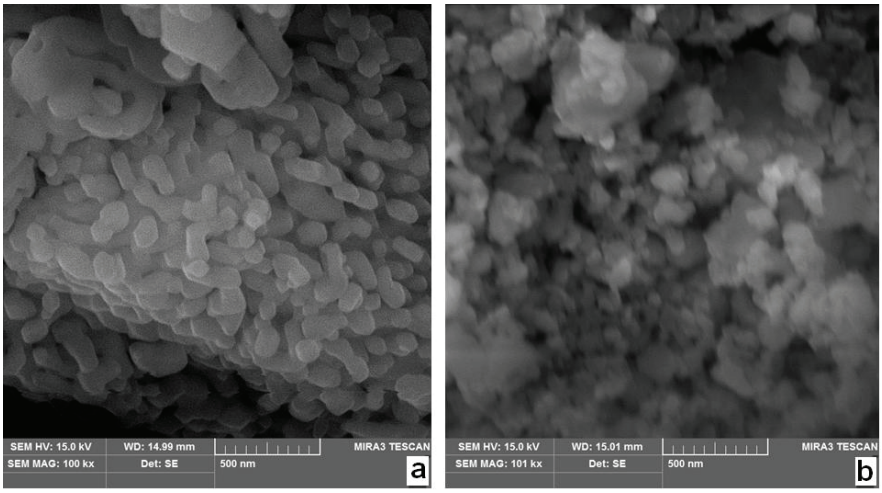

Fig. 1. The morphology of MgO powder (S = 9.4 m^2/g – a; S = 15.0 m^2/g – b).

The required amounts of carbonate eutectic and MgO were ground in an agate mortar and loaded into the instrument high-temperature accessory. The lack of any sedimentation of finely dispersed powders in molten $(Li_2CO_3–Na_2CO_3–K_2CO_3)_{eut}$ in a course of measurements was shown earlier.[8]

To analyze the changes of the physicochemical properties of the heterogeneous systems containing solid particles of different morphology with different geometrical parameters (specific surface area, crystallites average size) we used the approach suggested earlier.[11] The effective thickness (d) of the salt phase interlayer between MgO particles was taken into account. Parameter d was calculated according to the ratio:

$$d = \frac{V_{\text{eut}}}{Sm_{\text{MgO}}} \quad (1)$$

where V_{eut} is the salt composition volume and m_{MgO} is the MgO weight.

RESULTS AND DISCUSSION

DSC studies

DSC curves of the $(Li_2CO_3–Na_2CO_3–K_2CO_3)_{eut}$/MgO nanopowder heterogeneous systems with MgO concentrations up to 70 vol. % are depicted in Fig. 2. It was found that the melting point T_m and melting enthalpy ΔH reduced with an increase of the MgO nanopowder content in the system. This fact accounts for the influence of the salt – oxide interphase boundary on the thermodynamic parameters of ionic salt.

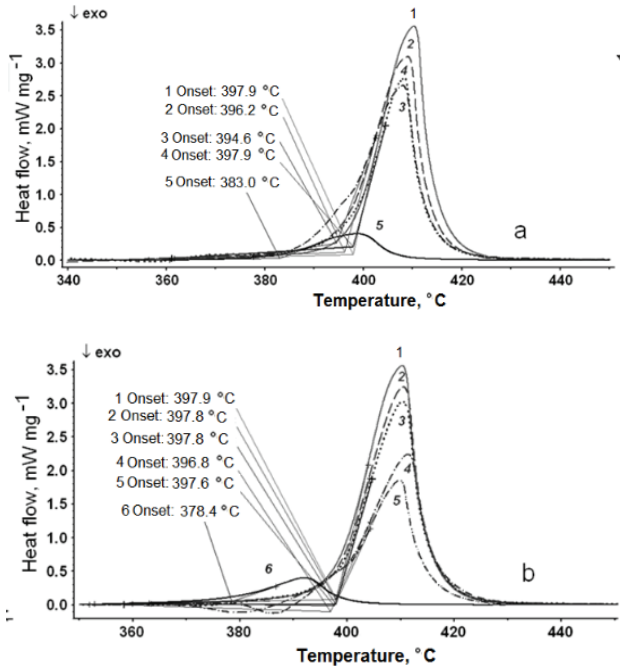

Fig. 2. DSC curves of the $(Li_2CO_3–Na_2CO_3–K_2CO_3)_{eut}$/MgO heterogeneous systems, MgO (vol. %): 1 – 0; 2 – 4.8; 3 – 11.1; 4 – 29.7; 5 – 70.1; S = 9.4 m^2/g – a; 1 – 0; 2 - 4.9; 3 – 8.9; 4 – 19.1; 5 – 28.6; 6 – 68.8; S = 15.0 m^2/g – b.

Fig. 3 demonstrates the dependences of obtained melting points (T_m) and normalized melting enthalpies (ΔH_{norm}) on the effective thickness d. Here ΔH_{norm} defined as $\Delta H_{norm} = \Delta H/\Delta H_{eut}$. From Fig. 3 we see that at d less than 100 nm, both the T_m and ΔH_{norm} of the salt phase in the heterogeneous system decreased drastically.

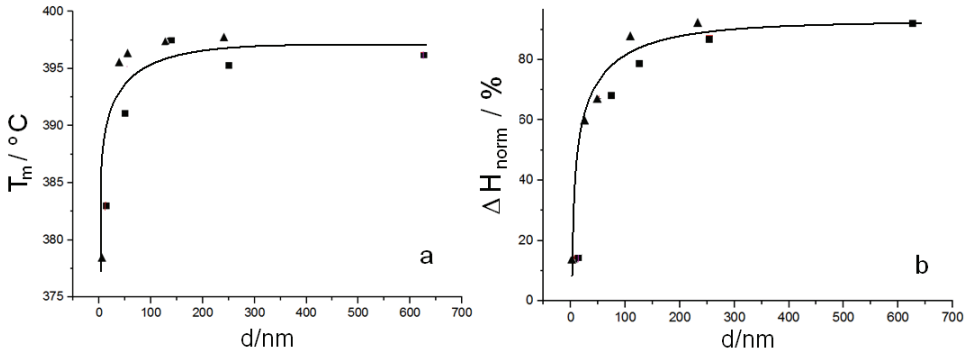

Fig. 3. Melting points (a) and the normalized melting enthalpies (b) of the salt phase in the heterogeneous system $(Li_2CO_3–Na_2CO_3–K_2CO_3)_{eut}$/MgO ($S$ = 9.4 m^2/g (squares), S = 15.0 m^2/g (triangles)).

At the temperatures below T_m the studied heterogeneous system may be analyzed as a nanocomposite,[16] which is composed of the alkali metal carbonates matrix and MgO powder filler. The interphase boundaries are known to contribute to the crystal defectiveness, which causes changes in thermodynamic parameters of phase transitions. In particular, the values of melting points and melting enthalpy provide information on the crystal disorder in near of melting temperature.[16] A drastic decrease of the T_m and ΔH_{norm} of the ionic salt in nanocomposite (Fig. 3) may be associated with the increase in defects concentration in the alkali metals carbonates crystalline lattice. It is important to note, that the effect does not depend on morphology and size of MgO particle, but only on effective thickness of the salt phase interlayer between MgO particles, which emphasizes its versatility to describe the physicochemical properties of composites ionic salt––oxide filler.

Electrical conductivity

The next stage of our work was devoted to the determination of the specific electrical conductivity of the $(Li_2CO_3–Na_2CO_3–K_2CO_3)_{eut}$/MgO heterogeneous system with the magnesium oxide concentration within the interval of 0 to 50 vol. %. The obtained experimental results are presented in Fig. 4a. In all cases the conductivity decreases with an increase of the solid content. Thus the specific conductivity reduces at the order of magnitude when volume fraction of MgO is equal 40 vol. %. The temperature dependence of the specific electrical conductivity, σ, can be approximated by linear equation as follows:

$$\ln \sigma = -E_a/RT + A \quad (2)$$

where E_a is the activation energy, R is the universal gas constant, A is the constant. The obtained dependencies are shown in Fig. 4b. Therefore, the values of E_a can be calculated, and in Fig. 5 presented the dependences of E_a on the effective

thickness of the carbonate melt interlayer between MgO particles (*d*). From Fig. 5 we see that at *d* less than 100 nm the activation energy of the specific electrical conductivity increase drastically. Returning to the data on T_m and ΔH_{norm}, it may be suggested that in $(Li_2CO_3–Na_2CO_3–K_2CO_3)_{eut}$/MgO heterogeneous system *d* = 100 nm is the boundary thickness of the salt phase between MgO particles, and for lesser values *d* the properties change significantly.

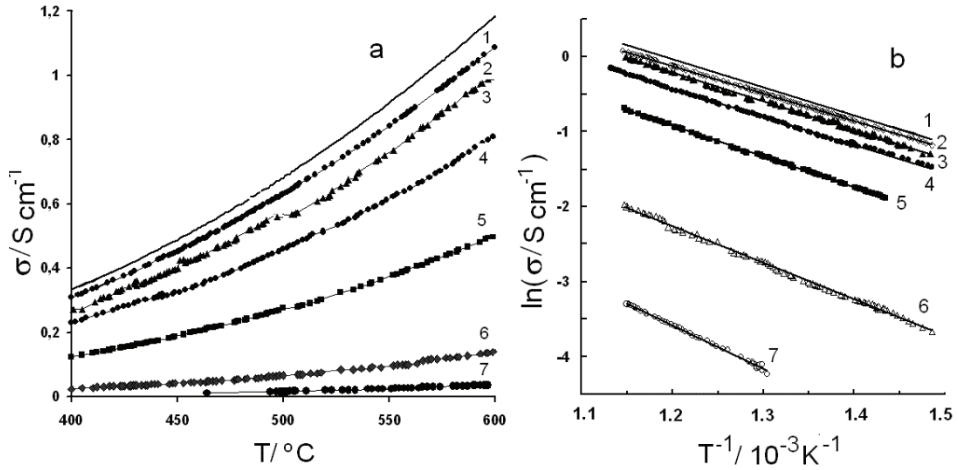

Fig. 4. Temperature dependences of the specific electric conductivity of the $(Li_2CO_3–Na_2CO_3–K_2CO_3)_{eut}$/MgO heterogeneous systems, MgO (vol. %): 1 – 0; 2 – 4.93; 3 – 9.90; 4 – 19.44; 5 – 29.45; 6 – 39.38; 7 – 49.52.

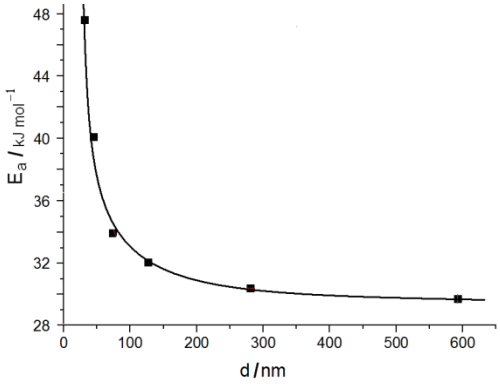

Fig. 5. Variation of the activation energy of the electrical conductivity with the effective average thickness of liquid phase for $(Li_2CO_3–Na_2CO_3–K_2CO_3)_{eut}$/MgO heterogeneous system.

The obtained data demonstrate that the charge transfer process near the solid phase particles surface is hindered and that there is an interaction between a disperse filler (solid MgO particles) and dispersing medium (molten carbonate eutectic). To specify the nature of this interaction we used the Raman spectroscopy.

Raman spectra

Raman spectra of molten $(Li_2CO_3–Na_2CO_3–K_2CO_3)_{eut}$ and $(Li_2CO_3–Na_2CO_3–K_2CO_3)_{eut}$ melt/MgO heterogeneous system with the magnesium oxide concentration up to 70 vol. % were qualitatively similar. Fig. 6 shows a typical spectrum of the $(Li_2CO_3–Na_2CO_3–K_2CO_3)_{eut}$ melt/MgO heterogeneous system. According to the selection rule, crystals of the *Fm3m* symmetry, such as magnesium oxide, have no the vibrational bands in the Raman spectra.

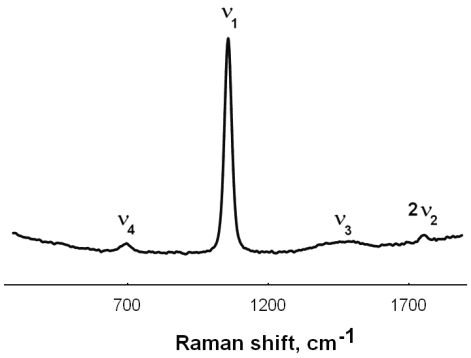

Fig. 6. Raman spectrum of the $(Li_2CO_3–Na_2CO_3–K_2CO_3)_{eut}$ melt/MgO heterogeneous system, 500 °C.

A strong band corresponding to fully symmetric stretching vibration ν_1 of CO_3^{2-} was observed at 1065 cm^{-1}. A weak band for bending vibration ν_4 near 700 cm^{-1}; a broad split band with maxima at 1390 and 1495 cm^{-1} for asymmetric stretching vibration ν_3; and overtone $2\nu_2$ near 1760 cm^{-1} of CO_3^{2-} were observed. Splitting of the ν_3 band into two components indicated that the symmetry of the CO_3^{2-} − anion reduced from D_{3h} to C_{2v}.[17] We found no bands point to the chemical interaction of magnesium oxide and $(Li_2CO_3–Na_2CO_3–K_2CO_3)_{eut}$ melt even with the long-term (4–5 h) exposure of $(Li_2CO_3–Na_2CO_3–K_2CO_3)_{eut}$ melt/MgO systems at 400–600 °C.

The XRD of the $(Li_2CO_3\text{-}Na_2CO_3\text{-}K_2CO_3)_{eut}$/MgO heterogeneous system after the high-temperature spectral experiments demonstrated the presence of $(Li_2CO_3–Na_2CO_3–K_2CO_3)_{euc}$ salt and MgO phases (Fig. 7).

However, we noticed a difference in the profiles of the vibration band ν_1 of the $(Li_2CO_3–Na_2CO_3–K_2CO_3)_{eut}$ melt and $(Li_2CO_3–Na_2CO_3–K_2CO_3)_{eut}$ melt/MgO heterogeneous systems: for molten $(Li_2CO_3–Na_2CO_3–K_2CO_3)_{eut}$ it was found to be symmetrical and to be well described by the Gaussian function (Fig. 8 (1)), while for $(Li_2CO_3–Na_2CO_3–K_2CO_3)_{eut}$ melt/MgO heterogeneous system ν_1 band profile is asymmetric because of the appearance of the additional high-frequency compound (Fig. 8, band C). In addition, under isothermal conditions the relative intensity of the high-frequency component (Fig. 8, band C) in the ν_1 band profile increases as the oxide phase specific surface area increase (Fig. 8 (2, 3)).

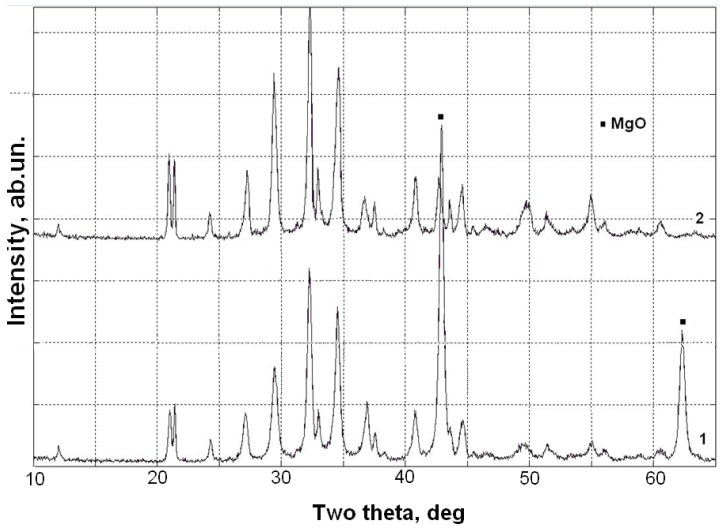

Fig. 7. XRD analysis (20 °C) of the $(Li_2CO_3–Na_2CO_3–K_2CO_3)_{eut}$/MgO heterogeneous system, MgO (vol. %): 1 – 70; 2 – 0.

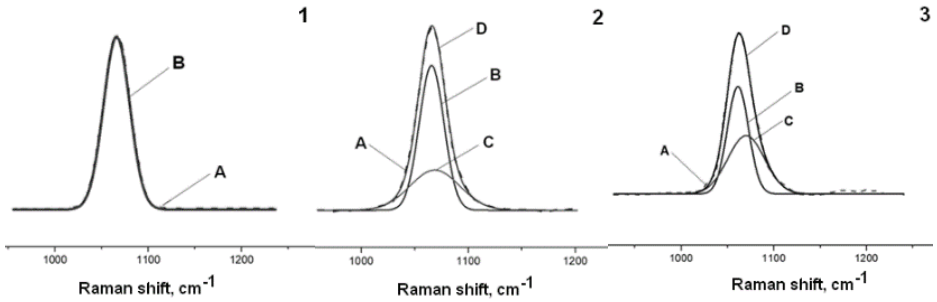

Fig. 8. Envelope of CO_3^{2-} vibrational band ν_1 in the Raman spectrum of $(Li_2CO_3–Na_2CO_3–K_2CO_3)_{euc}$ melt at 500 °C: experimental spectrum (A) and Gaussian approximation (B) of band – 1; envelope of the ν_1 band for $(Li_2CO_3–Na_2CO_3–K_2CO_3)_{eut}$ melt/MgO system, 70 vol. % MgO, S = 9.4 m^2/g – 2; S = 15.0 m^2/g – 3: experimental spectrum (A), Gaussian deconvolution components (B, C), and additive curve of *B* and *C* (D).

Previously was shown[18] that strong low-frequency component of the ν_1 band (Fig. 8, band B) for the disperse system $(Li_2CO_3–Na_2CO_3–K_2CO_3)_{eut}$ melt/MgO nanopowder is the ν_1 band of the carbonate ion in melt bulk, while a high-frequency component in the ν_1 band profile (Fig. 8, band C) associated with the CO_3^{2-}, adsorbed at the solid phase particle surface.[18,19] That is why the relative intensity of the high-frequency component in the ν_1 band increases as the oxide phase specific surface area increase (Fig. 8 – 2, 3).

Salt anions adsorbed on nanopowder-particle surfaces formed solvate shells that should have considerably affected the physicochemical properties of the

high-temperature disperse system $(Li_2CO_3–Na_2CO_3–K_2CO_3)_{eut}$ melt/MgO nanopowder. In particular, solvation of salt melt ions on the developed interface of solid phase particles hinders the process of electric charge transfer. Therefore, the a significant increase of the activation energy of electrical conductivity for the $(Li_2CO_3–Na_2CO_3–K_2CO_3)_{eut}$ melt/MgO nanopowder systems may be explained by the process of molten salt ions adsorption at the surface of the MgO solid phase particles.

CONCLUSION

DSC, AC impedance method and Raman spectroscopy were used to study the structure, conductivity and caloric melting effects of the $(Li_2CO_3–Na_2CO_3–K_2CO_3)_{eut}$ melt/MgO heterogeneous systems.

The data on the thermodynamic parameters of composite systems with MgO concentration up to 70 vol. % has been obtained by the DSC method. The anomalous decrease in the melting point and normalized melting enthalpy were observed at the values of effective thickness of the salt interlayer between the oxide particles below than 100 nm. The fall in the melting point from 398 to 378 °C and a normalized enthalpy of melting by 75 % was found.

The specific electrical conductivity of the heterogeneous systems based on the molten carbonate eutectic and finely MgO powder in the temperature range of 400–600 °C and magnesium oxide concentration up to 50 vol. % has been investigated. A significant increase in the activation energy of electrical conductivity from 30 to 48 kJ/mol was found when the thickness of the carbonate melt interlayer between magnesia particles became less than 100 nm.

The appearance of an additional vibrational band of the carbonate at 1075 cm^{-1} was found in the Raman spectrum of the heterogeneous system. The band is shifted by 10 cm^{-1} to higher frequencies compared to the vibrational band of the carbonate anion in the melt bulk. This is due to the Coulomb interaction of the carbonate anion and the Mg^{2+} in the surface layer of the magnesium oxide particles.

The data obtained by the *in situ* Raman spectroscopy method proved that the peculiarities of the electrical conductivity of the molten $(Li_2CO_3–Na_2CO_3–K_2CO_3)_{eut}$/MgO heterogeneous system are caused by the electrolyte ions adsorption at the surface of the solid phase particles.

ИЗВОД

ФИЗИЧКОХЕМИЈСКЕ ОСОБИНЕ ХЕТЕРОГЕНОГ СИСТЕМА $Li_2CO_3–Na_2CO_3–K_2CO_3$/MgO

IRINA D. ZAKIRYANOVA, ELENA V. NIKOLAEVA и IRAIDA V. KORZUN

Institute of High-Temperature Electrochemistry, 20 Akademicheskaya Street, 620066 Yekaterinburg, Russia

Истражена је структура, проводност, тачке топљења и калоријски ефекти топљења хетерогене смеше растопа $(Li_2CO_3–Na_2CO_3–K_2CO_3)_{eut}$ и MgO нанопраха са концентра-

цијом MgO до 70 % запремине. За карактеризацију узорака коришћен је широк спектар метода (DSC, XRD, BET, скенирајући електронски микроскоп високе резолуције, AC импеданција, IC и Раманска спектроскопија). Показано је да постоји нагли пад вредности тачака топљења соли и нормализоване енталпије фазног прелаза хетерогеног система када је ефективна дебљина међуслоја соли између MgO честица мања од 100 nm. Енергија активације електричне проводљивости се повећава са смањењем ефективне дебљине међуслоја фазе растопа између MgO честица. Истраживање је показало да не постоји хемијска интеракција између MgO и карбонатног растопа при температурама од 400–600 °C. *In situ* Раманска спектроскопија система растоп $(Li_2CO_3–Na_2CO_3–K_2CO_3)_{eut}$/MgO нано-прах је показала солвацију чврстих честица јонима растопљених соли.

(Примљено 1. фебруара, ревидирано 24. фебруара, прихваћено 15. априла 2023)

REFERENCES

1. R. Remick, D. Wheeler, *Molten Carbonate and Phosphoric Acid Stationary Fuel Cells: Overview and Gap Analysis*, National Renewable Energy Laboratory, Golden, CO, 2010 (https://www.nrel.gov/docs/fy10osti/49072.pdf)
2. M.W. Breiter, in *Electrochemical Processes in Fuel Cells,* Ed. M. Becke-Goehring, Springer, Berlin, 1969, p. 217 (https://doi.org/10.1007/978-3-642-46155-2_13)
3. S. Scaccia, *J. Mol. Liquids* **116** (2005) 67 (https://doi.org/10.1016/j.molliq.2004.07.078)
4. A. Kulkarni, S. Giddey, *J. Solid State Electrochem*. **16** (2012) 3123 (https://doi.org/10.1007/s10008-012-1771-y)
5. E. Antolini, *Ceram. Int.* **39** (2013) 3463 (https://doi.org/10.1016/j.ceramint.2012.10.236)
6. Zakir'yanova, I. Korzun, V. Khokhlov, V. Dokutovich, E. Nikolaeva, B. Antonov, *Russ. J. Appl. Chem.* **89** (2016) 1066 (https://doi.org/10.1134/S1070427216070041)
7. V. Dokutovich, V. Khokhlov, I. Zakir'yanova, *Int. J. Heat Mass Trans.* **119** (2018) 365 (https://doi.org/10.1016/j.ijheatmasstransfer.2017.11.132)
8. E. Nikolaeva, A. Bovet, I. Zakiryanova, *Zeitschrift Naturforsch., A* **73** (2018) 79 (https://doi.org/10.1515/zna-2017-0222)
9. M. Mizuhata, T. Ohashi, A. Béléké, *Int. J. Hydrogen Energy* **37** (2012) 19407 (https://doi.org/10.1016/j.ijhydene.2011.09.109)
10. M. Mizuhata, Y. Harada, G. Cha, A. Béléké, S. Deki, *J. Electrochem. Soc*. **151** (2004) 179 (https://doi.org/10.1149/1.1688798)
11. M. Mizuhata, A. Béléké, H. Watanabe, Y. Harada, S. Deki, *Electrochim. Acta* **53** (2007) 71 (https://doi.org/10.1016/j.electacta.2007.06.020)
12. R. Jenkins, R. Snyder, *Introduction to X-ray Powder Diffractometry*, John Wiley & Sons, New York, 1996 (https://doi.org/10.1002/9781118520994)
13. I. Zakir`yanova, E. Nikolaeva, A. Bove, *J. Appl. Spectrosc.* **81** (2015) 919 (https://doi.org/10.1007/s10812-015-0029-8)
14. I. Zakir′yanova, P. Arkhipov, D. Zakir′yanov, *J. Appl. Spectrosc*. **82** (2016) 920 (https://doi.org/10.1007/s10812-016-0205-5
15. G. J. Janz, *J. Phys. Chem. Ref. Data* **17** (1988) 3 (https://srd.nist.gov/JPCRD/jpcrdS2Vol17.pdf)
16. A. Ulihin, N. Uvarov, *ECS Trans*. **16** (2009) 445 (https://doi.org/10.1149/1.3242260)
17. K. Nakamoto, *Infrared and Raman Spectra of Inorganic and Coordination Compounds: Part A: Theory and Applications in Inorganic Chemistry,* John Wiley & Sons, New York, 2009 (https://doi.org/10.1002/9780470405840)

18. I. D. Zakir′yanova, *J. Appl. Spectr.*, **85** (2018) 611 (https://doi.org/10.1007/s10812-018-0694-5)
19. Béléké, M. Mizuhata, S. Deki. *Vibr. Spectrosc.* **40** (2006) 66 (https://doi.org/10.1016/j.vibspec.2005.07.002).